Single-channel EEG classification of sleep stages based on REM microstructure

Overturning Risk of Furniture in Earthquake Affected Areas

G. P. Cimellaro[1], M. Domaneschi[*1], Bing Qu[2]

[1] *Politecnico di Torino - DISEG, Turin, Italy*

[2] *California Polytechnic State University, San Luis Obispo, CA, USA*

ABSTRACT.

The main aim of this study is to develop a new straightforward approach to assess the overturning risk. The proposed formula is based on geometrical parameters of the furniture and the seismic intensity measures. In particular, the equation is identified by fitting the data obtained by the Housner's mechanical model from literature.

The new equation is compared with the model of Kaneko and Hayashi that, by the authors knowledge, is the only existing formulation in the literature to assess the overturning risk of furniture so far. Furthermore, to evaluate the consistency of the proposed formula, a comparison with literature experimental data has been also performed.

KEYWORDS: Furniture, Overturning, Earthquake, Risk, Damage

*Corresponding Author, Assistant Professor, email: marco.domaneschi@polito.it

1. INTRODUCTION

While moderate earthquakes may not induce significant structural damages, inside furniture sliding and overturning could injure occupants. Indeed, Sato et al. (2006) report that this type of injuries can be estimated around 40% of the total amount of earthquake-injured people. Besides, overturned objects have also an essential indirect effect during emergency by obstructing the evacuation paths (Figure 1).

As stated by Ishiyama (1982), when a rigid body is exposed to floor shaking due to an earthquake event, it may remain at rest when the intensity level is below a certain limit. However, when the floor motion overcomes that limit, the body may rock, slide, jump or may respond in a combination of these motions. Since this seminal paper a number of Japanese researchers was involved in the theme of furniture overturning (e.g. Winkler et al., 1995; Uematsu et al., 2000; Hamaguchi et al., 2004; Sato et al, 2006; 2011; Kuo et al. 2011; Shi et al., 2014).

The contribution by Housner (1963) is widely considered as the first systematic study about the dynamics and the rocking behavior of rigid bodies to base horizontal motion. After Housner, many authors have studied the dynamic motion of rigid bodies. Yim et al. (1980) and Ishiyama (1982) analyzed the rocking response of rigid blocks subjected to earthquakes through computer programs. Psycharis and Jennings (1983), and Spanos et al. (1984; 1986; 2001) investigated the effect of rigid or flexible foundation. In the work by Plaut et al. (1995) inclined planes are considered in the overturning problem. Hogan (1990; 1994) studied the response of a rigid block to horizontal simple harmonic forces at the theoretical level, explaining and confirming experimental results. Shenton (1996) investigated the boundary conditions governing the motion initiation. Uematsu et al. (2000) studied the rocking initiations factors with the experimental response on a shaking table. Rocking response to physically realizable trigonometric pulses is deepened in (Zhang and Makris, 2001), while relations of rocking spectrum to the kinematics characteristics of the ground motion is studied in (Makris and Konstantinidis, 2003). The use of distinct element method for columns

is also investigated in (Psycharis et al. 2000). Rocking response of a no-sliding rigid block subjected to a ground acceleration is studied in (Kounadis, 2010; 2013; 2015). The classical problem of rocking of a rigid block to near-fault earthquake motions is revisited by Voyagaki et al. (2012; 2013; 2014).

Ogino et al. (2015) analyzed the seismic behavior of cabinet and medical equipment through a finite element code and a penalty method. Asymmetric geometries are studied by Wittich and Hutchinson (2015). Boroschek and Iruretagoyena (2015) proposed an approach to control the overturning direction. Gesualdo et al. (2018a; 2018b) numerically and experimentally investigated the seismic protection of historic objects in museums and special equipment. The role of friction is also deepened in (Gesualdo et al., 2018c) and (Monaco et al., 2014).

Seismic risk analysis as reliable safety assessment method is widely employed in literature for regular buildings made of masonry (Kim and Baek, 2013; Preciado et al. 2015). Focusing on the explicit evaluation of the seismic overturning risk of furniture, the analytical model by Kaneko and Hayashi (2004), by the authors knowledge, is the only existing formulation in the literature. Estimated overturning ratios of furniture in a 14-story condominium due to the 2005 West Off Fukuoka Earthquake were compared to the actual observed effects to demonstrate the validity of the method (Nakamura et al., 2006). The results are reasonably in good agreement with the survey with a slight overestimation at low velocities of the low floors and a slight underestimation at high velocities of the high floors.

Considerable research has been dedicated to the use of different intensity measures (IM) that are commonly adopted in seismic vulnerability assessment frameworks. The peak ground acceleration (PGA) is one of the parameters most frequently used in earthquake engineering to express seismic hazard (Chen and Scawthorn 2003). An extensive literature review has been summarized in Pappas et al. (2017) that also investigate the efficiency of using the PGA and the peak ground velocity (PGV) as IM for the seismic vulnerability assessment of monolithic rocking columns, as suggested

77 before by Ishiyama (1984). The existence of an acceleration threshold for rocking of rigid bodies'
78 is discussed in Sorrentino et al. (2006).
79 In this paper, a new analytical expression to assess the risk of overturning using the peak ground
80 acceleration (PGA) as the intensity measure is presented. Rectangular shape elements with differ-
81 ent breadths and heights have been numerically tested using real earthquake floor motions of real
82 buildings monitored in real-time. Finally, the reliability of the proposed approach is validated
83 through a comparison with the results of shaking table tests.
84
85 Figure 1
86
87 **2. ESTIMATING THE RISK OF OVERTURNING**
88 ***2.1 HOUSNER'S EQUATION***
89 The model adopted in this paper is a rigid block on rigid base that can oscillate around two points
90 at the base during the rocking phase. The *center of gravity* corresponds to the *geometric center*,
91 where the weight force W is applied, and it is located at a distance r from any corner of the block
92 (Housner, 1963). Angle α is given by $tan(\alpha)=B/H$ where B and H are the base and height dimen-
93 sions respectively. Depending on the value of the base acceleration $\frac{d^2u_g}{dt^2}$ and the friction coeffi-
94 cient μ, the block translates with the ground, enters in rocking or sliding motion. The required
95 condition for the block to enter in rocking motion is $\mu > B/H$ (Aslam 1980, Scalia and Sumbatyan
96 1996).
97 In this study, the following assumptions have been adopted: (i) the coefficient of friction between
98 the block and its base is sufficiently large to prevent sliding at any instant during the rocking mo-
99 tion. (ii) Identical angular momentum on corners is assumed before and after the impact. (iii) No
100 vertical motion at the rocking point is assumed. (iv) The body and the support are assumed rigid.
101 (v) The response is planar.

When the block is subjected to a positive horizontal acceleration $\frac{d^2u_g}{dt^2}$ it can have first a negative rotation $\theta<0$. Then, if it does not overturn, it will eventually assume a positive rotation and so forth. The equations of motion are:

$$I_0\frac{d^2\theta}{dt^2}+mgr\sin\left(-\alpha-\theta\right)=-m\frac{d^2u_g}{dt^2}r\cos\left(-\alpha-\theta\right)\qquad\theta<0 \tag{1}$$

and

$$I_0\frac{d^2\theta}{dt^2}+mgr\sin\left(\alpha-\theta\right)=-m\frac{d^2u_g}{dt^2}r\cos\left(\alpha-\theta\right)\qquad\theta>0 \tag{2}$$

where $I_0=\frac{4}{3}mr^2$ is the rotational inertia. Equations (1) and (2) can be expressed in the compact form:

$$\frac{d^2\theta(t)}{dt^2}=-p^2\left\{\sin\left(\alpha\ sgn\left[\theta(t)\right]-\theta(t)\right)+\frac{d^2u_g}{dt^2}\frac{1}{g}\cos(\alpha\ sgn\left[\theta(t)\right]-\theta(t))\right\} \tag{3}$$

where

$$p=\sqrt{\frac{3g}{4r}} \tag{4}$$

is the frequency in [rad/sec] of the block and g the acceleration of gravity.

If the block remains at rest and then is subjected to a sudden constant acceleration $\frac{d^2u_g}{dt^2}$, it may or may not overturn depending on the intensity of the acceleration and its duration. For small angles of oscillation, the undeformed (at rest) and deformed configurations of the body coincides and the necessary condition for the initiation of motion can be defined by rotation equilibrium as $\frac{d^2u_g}{dt^2}\frac{1}{g}>\frac{B}{H}\approx\alpha$. Equations (1) and (2) are applicable when motion initiates and the overturning condition is reached when the angle $|\theta|=\pi/2$.

The problem is described as an inverted pendulum model, therefore the results are independent from the mass, while the geometry exclusively controls the phenomenon. If the rigid body has a slender shape, the angle α is smaller and the overturning has more chances to be verified.

The Housner model has been implemented in MATLAB (2015) to solve the differential equations and then to compute the overturning risk. The differential equation belongs to the *stiff* category, because some terms can lead to a rapid variation in the solution, therefore the solution methods might be numerically unstable. A sensitivity analysis has been conducted by testing different ground motion inputs and different integration methods.

Figure 2

MATLAB allows different algorithms to solve a system of differential equations. The most effective functions for this problem are ODE45 and ODE23s that are both based on Runge-Kutta schemes, of order 4-5 and 2-3 respectively. The last one is designed specifically for solving stiff differential equations with a low order of accuracy and automatic time stepping. Relative error and the absolute error tolerance of the solvers are also value parameters that can drive results toward accurate solutions.

Figure 2a reports the input sine pulse function ($\ddot{u}_g = a_p \sin(\omega_p t)$ with p=2.14rad/s, w_p/p=5, α=0.25rad, H=0.9m) to evaluate the selected functions. Figures 2b and 2c describe the results of ODE45 and ODE23s algorithms respectively.

The reference responses as obtained by Zhang and Makris (2001) are shown in Figure 2d and are used for selecting the suitable algorithm. They represent the transition point between overturning and not-overturning, as the critical condition for the problem under investigation. The tested solvers have been required to identify the transition point. ODE23s algorithm has been selected with the following error parameters: *RelTol*=1e-05 and *AbsTol*=1e-07 (MATLAB, 2015).

2.2 KANEKO AND HAYASHI FORMULATION

In 2004 Kaneko and Hayashi conducted several seismic response analyses of different rectangular rigid bodies. The reference mechanical model can consider both sliding and deformability, so when the supporting point is in contact with the floor, springs, dashpots and slider are engaged in both horizontal and vertical directions. Their parameters have been adopted corresponding to a rigid support. The simplified equation of the overturning risk was then derived through a regression process using the log-normal distribution function as follows:

$$R = \begin{cases} \alpha \cdot \phi\left(\left(\ln PFA - \lambda_A\right)/\zeta_A\right), & F_f \le F_b \\ \alpha \cdot \phi\left(\left(\ln PFV - \lambda_V\right)/\zeta_V\right), & F_f > F_b \end{cases} \quad (5)$$

where PFV ([cm/s]) and PFA ([cm/s^2]) are the peak floor velocity and acceleration respectively, α the slide resistant coefficient ([0,1]) that is function of the ratio *B/H* and the friction coefficient (assumed sufficiently high to prevent sliding during rocking), ϕ the normal distribution function. The mean values of the acceleration and the velocity λ_A and λ_V are given by the following relations:

$$\lambda_A = \ln\left(\left(B/H\right)g \cdot \left(1 + B/H\right)\right); \quad \lambda_V = \ln\left(10B/\sqrt{H} \cdot \left(1 + B/H\right)^{2.5}\right) \quad (6)$$

ζ_A and ζ_V are the corresponding standard deviations (Kaneko and Hayashi 2004). the furniture boundary frequency and the equivalent floor frequency F_b and F_f ([Hz]) are given by:

$$F_f = PFA/\left(2\pi PFV\right), \quad F_b = 15.6/\sqrt{H} \cdot \left(1 + B/H\right)^{-1.5} \quad (7)$$

H and *B* in [cm] are the furniture breadth and height. In Kaneko and Hayashi (2004) the following classification is determined: *Low risk* if $R<0.03$, *Medium risk* if $0.03<R<0.3$, *High risk* $0.3<R<0.7$, *Very high* risk if $R>0.7$.

3. APPLICATION TO MONITORED BUILDINGS

3.1 SIMPLIFIED APPROACH

171 The overturning risk of furniture is evaluated in 50 real-time monitored buildings in California
172 (CESMD 2017) subjected from 1987 to different earthquakes (Table 1).
173
174 Table 1
175
176 Figure 3
177
178 Overturning risk analyses have been performed by employing Kaneko and Hayashi (2004) formu-
179 lation using floor accelerations. For each one of the 50 cases, the furniture has been placed with
180 the shortest side parallel to the direction of the sensor that recorded the floor motion (Figure 3a).
181 Figure 3b shows the results in terms of risk of overturning *R* for each ID case in Table 1 where
182 three buildings (ID 003, 004, 005) highlight *very high* overturning risk, in particular at the top
183 floor. However, it is also worth underlining how, sometimes, the discrepancies in terms of *R* be-
184 tween two channels from sensors located at the same floor are very large. E.g., the results obtained
185 for ID 003 shows a strange behavior at the roof floor: one channel determines a very high *R*, while
186 for the others signals on the same floor the risk is rather negligible. The same consideration can be
187 done also for building ID 004.
188
189 ### *3.2 Detailed Analysis*
190 Because of the highlighted discrepancies, a detailed analysis using Housner's formulation has been
191 performed for the three buildings where overturning risk was the highest. The overturning risk is
192 re-evaluated through direct integration and the results are compared to those computed by Kaneko
193 and Hayashi approach.
194

3.2.1 Buildings description

The office building ID 003 (Figure 4a) is placed in San José (California). The building is founded on rocks and is part of five rectangular structures (1 spine and 4 wings), separated by expansion joints. It was equipped with 10 accelerometers, placed on three levels in the building and at a reference free-field station. The vertical load carrying system is made of concrete over steel deck supported by steel frames, while the lateral force resisting system consists in a moment resisting steel frame.

Building ID 004 (Figure 4b) is an Hospital located in Palm Spring, California. The building has a rectangular plan and is founded on rocks. It was equipped with 13 accelerometers, placed on four levels in the building. The vertical load carrying system is made of reinforced concrete slabs, while the lateral force resisting system consists in a moment resisting steel frame.

Figure 4

South of San Francisco office building ID 005 has a rectangular plane as shown in Figure 4c. It was equipped with 11 accelerometers, placed on four levels in the building. The vertical load carrying system is made of a moment-resistant steel frame, as the lateral force resisting one. The foundation is made of 15-21 m deep reinforced concrete piles.

3.2.2 Comparison of numerical models to assess risk of overturning

The estimation of the overturning risk using the direct integration analysis is computationally demanding and for every channel, it is necessary to solve step by step the Housner's differential equation. The results of the comparison between the *simplified* (Kaneko and Hayashi) and the *direct integration* (Housner) approaches are presented in Table 2. The same table reports also the *proposed formulation* outcomes that will be discussed at next Section 4.

The risk of overturning obtained with the direct integration method has been computed for the adopted deterministic model of Housner through a Montecarlo simulations where the input has been limited to a fixed number of events (100 earthquake records) that are spectrum compatible with the recorded acceleration signal. Figure 5 provides as example the ACCHAN04 at building 003 case. The numerical results obtained through the direct integration method show that the risks of overturning for furniture located on the same floor are coherent. This can be noticed at the fourth floor of the building 003, as well as at the fifth floor of the building 004, where the discrepancies observed with the simplified approach are resolved with the direct integration one. Furthermore, from the last approach, higher overturning risks arise.

Figure 5

Table 2

3.2.3 Dependency on the furniture slenderness

The slenderness of the furniture plays a crucial role in the overturning phenomena. Therefore, the comparison between the simplified approach and the Housner's formulation through direct integration has been extended by ranging the dimension of the base of the furniture. The overturning risk is presented in Figure 6, where the base of the furniture is shown in abscissa, while in ordinate the peak floor accelerations are presented. The contour plots in Figure 6 have been drawn using the following procedure: (i) the risk of overturning for all the channels inside the considered building is evaluated using the procedure described in previous section; (ii) the channel with the higher risk of overturning is selected for each building; (iii) the selected channel records are scaled to different values of PFA to be used in the risk analyses.

Figure 6

The discrepancies highlighted by the simplified approach in Table 2 are confirmed also in Figure 6 where an irregular trend is marked, with respect to the consistent variation of the direct integration outcomes.

The irregular behavior of Kaneko and Hayashi formulation is clearly visible in all three buildings. An explanation of this trend is due to the presence of a switch operator in Equation 5. It depends on the equivalent floor frequency value and the furniture boundary frequency value, respectively F_f and F_b [Hz]. The first one depends on the ground motion characteristic while the second one depends on the geometric characteristics of the furniture. If the floor frequency is higher than the furniture frequency, the overturning risk is a function of the peak floor acceleration. Conversely, if the furniture frequency is higher than the furniture frequency, the overturning risk is a function of the peak floor velocity.

The results obtained with Housner's formulation show a more regular trend. Considering the intrinsic nonlinearities of the problem and the analytical formulation, the obtained results can be considered more accurate. Furthermore, as expected, the Housner's formulation presents comparable results at different locations on the same floor.

4. PROPOSED FORMULATION

Because of the highlighted discrepancies between the simplified formulas proposed by Kaneko and Hayashi, a new equation has been proposed by fitting the data obtained by the Housner's mechanical model.

The aim of this new formula is to provide a way to estimate the risk of furniture overturning inside a building reducing the computational time with respect to the direct integration method and achieving consistent and reliable results. The proposed formulation includes the major variables of the problem, as the furniture's dimensions and the peak floor acceleration.

Several polynomial functions have been analyzed with a surface fit process that fits and ranks a series of equations, such as polynomials, to find the best equation that describe the reference values. At the end of the process the following Taylor Series Polynomial has been selected:

$$z = a + \frac{b}{x} + cy + \frac{d}{x^2} + ey^2 + f\frac{y}{x} \tag{8}$$

Taylor Series approach is a worthy approximation for a continuous function as that one herein assumed. Indeed, the continuity of the problem can be theoretically evaluated through the analytical approaches for the hazard modeling (e.g., Cao et al. 1996, Crowley and Bommer 2006) and the fragility functions of mechanical components (e.g., Petrone et al., 2017 for blocks). Following the PEER (Pacific Earthquake Engineering Research) approach and the discussion by Der Kiureghian (2005), the computation of failure probability for a mechanical component under seismic loading can be cast into the "PEER probability approximation" formula (Perotti et al., 2013). The continuity of the problem has been also numerically evaluated for the proposed approach by analyzing the fitting surface.

Connected to the overturning behavior, which represents a potential resulting phase of the rigid body motion, is the preliminary phase of rocking response that was deeply investigated (numerically) by Lin et al. in 90s (e.g., Yim and Lin, 1991). Contrary to previous belief, the lack of stable periodic responses does not necessary imply overturning and quasi-periodic and chaotic responses may result. Furthermore, it has been also demonstrated that the rocking response of rigid objects can be very sensitive to the system parameters and the ground-motion details. It means that some experiments could result unrepeatable and probabilistic trends can only be established with a large sample size.

Equation (8) has been re-written to include the major variables of the problem:

$$OR = a + \frac{b}{(B/H)} + c\cdot(PFA) + \frac{d}{(B/H)^2} + e\cdot(PFA)^2 + f\frac{(PFA)}{(B/H)} \tag{9}$$

where variables *PFA* [cm/sec2], *H* [cm] and *B* [cm] remain the same previously described. The six coefficients *a, b, c, d, e, f* have been estimated through Ordinary Least Squared method over the

recorded data. The overturning risk *R* for the three buildings evaluated with Housner's formulation have been used as target to determine the unknown coefficients. The final coefficients at the end of the process are the following: a = -0.97758451, b = 0.30856415, c = 0.0032112873, d = -0.018590461, e = -0.000001941, f = -0.00010152672. Figure 7 reports the comparison between the results of the Housner's model and the proposed formula, where in the X-axis is the ratio *B/H* and in the Y-axis, are the recorded peak floor accelerations in the steel buildings.

Figure 7

Figure 8

Table 2 reports the comparison of overturning risk computed by the different formulations for all buildings. The overturning risk evaluated with the proposed formulation is homogeneous inside a single floor and the number of overturning phenomena is consistent with the number of overturning determined using Housner's model. It can be noticed that the proposed formulation in Figure 8 shows regular trend, consistently reproducing the Housner's results (Figure 6) for different furniture slenderness.

5. COMPARISON WITH EXPERIMENTAL DATA

To evaluate the consistency of the proposed formula, a comparison with literature experimental data (Purvance et al. 2008) has been performed. The tests were implemented on an unidirectional shaking table and consisted of scaling acceleration time histories from 0.1g, in 0.025g increments, to the point where each block overturned at least once. The overturning responses of several symmetric blocks have been investigated (Table 3): the wooden blocks W1, W2, and W3 have the exact dimensions of the aluminum blocks AL1, AL2, and the granite block G, respectively. The

blocks IB0, IB2, and IB4 consist of ~1.2m tall steel I-beam sections with masses symmetrically affixed to vary their geometries. Additional details can be found in (Purvance et al. 2008).

The results of the comparison are detailed in the same Table 3 with objects dimensions, the overturning PGA in terms of mean, maximum and minimum values over ten tests for each sample. It can be noted a satisfactory compatibility between the laboratory overturning conditions and the estimated overturning risk (*very high* for mean and maximum PGAs, *high* for minimum PGAs.

6. CONCLUDING REMARKS

A simplified formula to locate and measure the risk of overturning for a rigid block in buildings is identified following a surface fit process. The proposed approach is compared with two models, the Housner and the simplified formulation by Kaneko and Hayashi. The overturning risk has been evaluated using real-time monitored buildings and different furniture dimensions. Moreover, the consistency of the new formula has been evaluated through a comparison with the results of shaking table tests on different rigid blocks.

With respect to the state of the art on overturning risk assessment, the new formula gives more consistent results, clearly stable and homogeneous on specific floors of the structure where, on the contrary, the Kaneko and Hayashi formulation highlights unrealistic discrepancies. The proposed formula has also proven to be able to locate different risk of overturning at different floors of a given building.

The main advantage of the proposed formulation is also to reduce the computational time with respect to direct integration methods without losing accuracy in the results.

ACKNOWLEDGEMENTS

The authors declare no conflict of interest in preparing this article.

REFERENCES

Aslam M, Godden WG, and Scalise DT (1980). Earthquake rocking response of rigid bodies. *Journ. Engrg. Mech. Div., ASCE*, 106(2):377-392.

Boroschek R, and Iruretagoyena A (2015). Controlled overturning of unanchored rigid bodies. *Earthq Eng Struct D*, 35(6):695-711.

Cao T, Petersen MD, and Reichle MS (1996). Seismic Hazard Estimate from Background Seismicity in Southern California. *Bulletin of the Seismological Society of America*, 86 (5):1372-1381.

CEN (2004). Eurocode 8: Design of structures for earthquake resistance, Brussels, Belgium.

CESMD (2017). http://www.strongmotioncenter.org, Accessed June 3 2017.

Chen WF, and Scawthorn C (2003). *Earthquake Engineering Handbook*, CRC Press, Boca Raton, FL, USA.

Cimellaro GP, Chiriatti M, Reinhorn AM, and Tirca L (2012). Emilia Earthquake of May 20th, 2012 in Northern Italy: rebuilding a resilient community to multiple hazards. *MCEER Technical Report –MCEER-12-0009*, MCEER, State University of New York at Buffalo (SUNY), Buffalo, New York.

Cimellaro GP, Chiriatti M, Roh H, and Reinhorn AM (2014). Seismic performance of industrial sheds and liquefaction effects during May 2012 Emilia Earthquakes sequence in Northern Italy. *Journal of Earthquake and Tsunami*, 8(2):23.

Crowley H, And Bommer JJ (2006). Modelling Seismic Hazard in Earthquake Loss Models with Spatially Distributed Exposure. *Bulletin of Earthquake Engineering*, 4:249–273.

Der Kiureghian A (2005). Non-ergodicity and PEER's framework formula. *Earthquake Engineering and Structural Dynamics*, 34:1643–1652.

Gesualdo A, Iannuzzo A, and Monaco M (2018a). Rocking behaviour of freestanding objects. *Journal of Physics: Conference Series*, 1141(1):012091.

Gesualdo A, Iannuzzo A, Minutolo V, Monaco M (2018b). Rocking of freestanding objects: Theoretical and experimental comparisons. *Journal of Theoretical and Applied Mechanics*, 56 (4):977-991.

Gesualdo A, Iannuzzo A, Monaco M, and Penta F (2018c). Rocking of a rigid block freestanding on a flat pedestal. *Journal of Zhejiang University: Science A*, 19(5):331-345.

Hamaguchi H, Higashino M, Shimano Y, and Tsubaki H (2004). Simple Prediction Method of Furniture Damages during Earthquakes. *13th World Conference on Earthquake Engineering*, 745.

Hogan SJ (1990). The many steady state responses of a rigid block under harmonic forcing. *Earthquake Engineering & Structural Dynamics*, 19(7):1057-1071.

Hogan SJ (1994). Slender rigid block motion. *Journal of Engineering Mechanics*, 120 (1):11-24.

Housner G (1963). The beaviour of inverted pendulum structures during earthquakes. *Bulletin of the Seismiological Society of America*, 53(2):403-417.

Kaneko M, and Hayashi Y (2004). A proposal for simple equations to express a relation between overturning ratios of rigid bodies and input excitation. *13th World Conference on Earthquake Engineering (13WCEE).* Vancouver, Canada.

Kim J, and Baek D (2013). Seismic risk assessment of staggered wall system structures. *Earth-quakes and Structures*, 5(5):607-624.

Kounadis A.N. (2010). On the overturning instability of a rectangular rigid block under ground excitation. *Open Mechanics Journal*, 4(1):43-57.

Kounadis AN (2013). Parametric study in rocking instability of a rigid block under harmonic ground pulse: A unified approach. *Soil Dynamics and Earthquake Engineering*, 45:125-143.

Kounadis AN (2015). On the rocking-sliding instability of rigid blocks under ground excitation: some new findings. *Soil Dynamics and Earthquake Engineering*, 75:246-258.

Kuo KC, Suzuki Y, Katsuragi S, and Yao GC (2011). Shake table tests on clutter levels of typical medicine shelves and contents subjected to earthquakes. *Earthquake Engineering & Structural Dynamics*, 40(12):1367-1386.

Ishiyama Y (1982). Motions of Rigid Bodies and Criteria for Overturning by Earthquake Excitations. *Earthq Eng Struct D*, 10(5):635-650.

Makris N, and Konstantinidis D (2003). The rocking spectrum and the limitations of practical design methodologies. *Earthquake Engineering and Structural Dynamics*, 32(2):265-289.

Matlab (2015). Matlab R2015, The Mathworks.

Monaco M, Guadagnuolo M, and Gesualdo A (2014). The role of friction in the seismic risk mitigation of freestanding art objects. *Natural Hazards*, 73(2):389-402.

Nakamura Y, Kaneko M, Kambara H, and Tamura K (2008). Seismic Safety Evaluation Method for Buildings Contents. *Proceedings of the 14th World Conference on Earthquake Engineering*, S20-002.

Ogino H, Yamashita T, Kaneko M, and Isobe D (2015). Development of a finite element code to simulate behaviors of furniture under seismic excitation. *Journal of Structural and Construction Engineering*, 80(717):1687-1697.

Pappas A, Sextos A, da Porto F, Modena C (2017). Efficiency of alternative intensity measures for the seismic assessment of monolithic free-standing columns. *Bull Earthquake Eng*, 15:1635–1659.

Perotti F, Domaneschi M, and De Grandis S (2013). The numerical computation of seismic fragility of base-isolated NPP buildings. *Nucl Eng Des*, 262:189–200.

Petrone C, Di Sarno, L, Magliulo G, and Cosenza E (2017). Numerical modelling and fragility assessment of typical freestanding building contents. *Bulletin of Earthquake Engineering* 15:1609–1633

Plaut, R.H., Fielder, W.T., and Virgin, L.N. (1995). "Fractal behavior of an asymmetric rigid block overturning due to harmonic motion of a tilted foundation". *Chaos Soliton Fract*, 7(2):177–196.

Preciado, A., Ramirez-Gaytan, A., Salido-Ruiz, R.A., Caro-Becerra, J.L., and Lujan-Godinez, R. (2015). "Earthquake risk assessment methods of unreinforced masonry structures: Hazard and vulnerability". *Earthquakes and Structures, An Int'l Journal*. 9(4) :719-733.

Psycharis I, and Jennings PC (1983). Rocking of slender rigid bodies allowed to uplift. *Earthq Eng Struct D*, 11(1):57-76.

Psycharis IN, Papastamatiou DY, and Alexandris AP (2000). Parametric investigation of the stability of classic al columns under harmonic and earthquake excitations. *Earthquake Engineering and Structural Dynamics*, 29(8):1093-1109.

Sato T, Motosaka M, and Mano A (2006). Investigation of Human Injuries during the July 26, 2003 Northern Miyagi Earthquake with Focus on Furniture Overturning. *Journal of Natural Disaster Science*, 28(1):15-24.

Sato E, Furukawa S, Kakehi A, and Nakashima M (2011). Full scale shaking table test for examination of safety and functionality of base isolated medical facilities. *Earthquake Engineering & Structural Dynamics*, 40(13):1435-1453.

Scalia A, and Sumbatyan MA (1996). Slide rotation of rigid bodies subjected to a horizontal ground motion. *Earthq Eng Struct D*, 25(10):1139-1149.

Shenton HW (1996). Criteria for initiation of slide, rock, and slide-rock rigid-body modes. *J Eng Mech-ASCE*, 122(7):690-693.

Shi Y, Kurata M, and Nakashima M (2014). Disorder and damage of base isolated medical facilities when subjected to near fault and long period ground motions. *Earthquake Engineering & Structural Dynamics*, 43(11):1683-1701.

Sorrentino L, Masiani R, and Decanini LD (2006). Overturning of rocking rigid bodies under transient ground motions. *Structural Engineering and Mechanics*, 22(3):293-310.

Spanos PD, and Koh AS (1984). Rocking of rigid blocks due to harmonic shaking. *Journal of Engineering Mechanics*, 110(11), 1627-1642.

Spanos PD, and Koh AS (1986). Analysis of block random rocking. *Soil Dynamics and Earthquake Engineering*, 5(3):178-183.

Spanos PD, Roussis PC, and PC, Politis N (2001). Dynamic analysis of stacked rigid blocks. *Soil Dynamics and Earthquake Engineering*, 21 (7):559-578.

Uematsu T, Miyagi M, and Ishiyama Y (2000). Rocking motion and criteria for overturning of bodies on a floor comparison between analysis and experiment. *12th World Conference on Earthquake Engineering*, Auckland, New Zealand, 2313.

Voyagaki E, Mylonakis G, Psycharis IN (2012). Rigid block sliding to idealized acceleration pulses. *Journal of Engineering Mechanics*, 138(9):1071-1083.

Voyagaki E, Psycharis IN, Mylonakis G (2013). Rocking response and overturning criteria for free standing rigid blocks to single-lobe pulses. *Soil Dynamics and Earthquake Engineering*, 46:85-95.

Voyagaki E, Psycharis IN, Mylonakis G (2014). Complex response of a rocking block to a full-cycle pulse. *Journal of Engineering Mechanics*, 140(6), 04014024.

Winkler T, Meguro K, and Yamazaki F (1995). Response of rigid body assemblies to dynamic excitation. *Earthquake engineering & structural dynamics*, 24(10):1389-1408.

Wittich CE, and Hutchinson TC (2015). Shake table tests of stiff, unattached, asymmetric structures. *Earthq Eng Struct D*, 44(14):2425-2443.

Yim CS, Chopra AK, and Penzien J (1980). ocking response of rigid blocks to earthquakes. *Earthq Eng Struct D*, 8(6):565-587.

Yim SCS, and Lin H (1991). Nonlinear impact and chaotic response of slender rocking objects. *Journal of Engineering Mechanics*, 117(9):2079-2100.

Zhang J, and Makris N (2001). Rocking Response of Free-Standing Blocks under Cycloidal Pulses. *J Eng Mech-ASCE*, 127(5):473-483.

472 **Table 1**. Real-time monitored buildings and floor motion data

ID	Station	No. of Stories	Height (in.)	Earthquake	PGA (g) Transv.	PGA (g) Long.
001	Pasadena (Office bldg)	12	2016	Northridge, 17 Jan. 1994	0.135	0.234
002	Burbank (Commercial bldg)	6	990	Whittier, 1 Oct. 1987	0.17	0.23
003	San Jose (Office bldg)	3	594	LomaPrieta, 17 Oct. 1989	0.18	0.2
004	Palm Springs (Hospital)	4	954	Palm Springs, 8 July 1986	0.16	0.19
005	South San Francisco (Office bldg)	4	726	Loma Prieta, 17 Oct. 1989	0.16	0.14
006	Richmond (Office bldg)	3	554	Loma Prieta, 17 Oct. 1989	0.11	0.08
007	San Jose (Gov. Office bldg)	13	2527	Loma Prieta, 17 Oct. 1989	0.087	0.098
008	San Bernardino (Office bldg)	3	496	Landers, 28 June 1992	0.11	0.08
009	Burbank (Commerce bldg)	6	990	Sierra Madre, 28 June 1991	0.11	0.12
010	San Rafael (Hospital)	5	1110	Bolinas, 17 Aug. 1999	0.107	0.082
011	Pasadena (Office bldg)	12	2016	Whittier Narrows, 16 March 2010	0.045	0.11
012	San Bernardino (Office bldg)	3	496	San Bernardino, 08 Jan. 2009	0.1	0.08
013	San Bernardino (Commercial bldg)	9	1411	Landers, 28 June 1992	0.068	0.088
014	Pasadena (Office bldg)	12	2314	Northridge 17 Jan. 1994		
015	Pasadena (Office bldg)	12	2016	Chino Hills, 29 July 2008	0.08	0.06
016	San Bernardino (Hospital)	5	828	Northridge, 17 Jan. 1994	0.046	0.057
017	Redlands(Commercial bldg.)	7	1253	Landers, 28 June 1992	0.06	0.07
018	San Bernardino (Hospital)	5	828	Landers, 28 June 1992	0.08	0.08
019	Lancaster (Hospital)	5	942	Landers, 28 June 1992	0.08	0.05
020	Chatsworth (Commercial bldg)	2	482	Chino Hills, 29 July 2008	0.07	0.04
021	Long Beach (Office bldg)	7	1248	Whittier, 1 Oct. 1987	0.07	0.04
022	Lancaster (Hospital)	5	942	Landers, 28 June 1992	0.055	0.07
023	San Bernardino (Hospital)	5	828	Big Bear, 28 June 1992	0.06	0.07
024	Los Angeles (Residential bldg)	32	4214	Chino Hills, 29 Jul 2008	0.065	0.06
025	Long Beach (Gov. Office bldg)	15	3456	Whittier, 1 Oct. 1987	0.055	0.041
026	Long Beach (Gov. Office bldg)	15	3456	Inglewood, 17 May 2009	0.059	0.043
027	San Bernardino (Office bldg)	3	496	Chino Hills, 29 July 2008	0.052	0.047
028	Chatsworth (Commercial bldg)	2	482	Chatsworth, 09 Aug. 2007	0.04	0.046

029	San Jose (Gov. Office bldg)	13	2527	Morgan Hill, 24 April 84	0.039	0.036
030	San Jose (Office bldg)	3	594	Alum Rock, 30 Oct. 2007	0.034	0.027
031	Palm Springs (Hospital)	4	954	Calexico, 04 April 2010	0.04	0.02
032	San Bernardino (Hospital)	5	828	Chino Hills, 29 July 2008	0.0265	0.036
033	San Bernardino (Office bldg)	3	496	Lake Elsinore, 02 Sept. 2007	0.036	0.031
034	San Diego (Commercial bldg)	22	3804	Calexico, 04 April 2010	0.034	0.026
035	Palm Springs (Hospital)	4	954	Borrego Springs, 07 July 2010	0.03	0.03
036	Los Angeles (Residential bldg)	32	4214	Whittier Narrows, 16 March 2010	0.028	0.033
037	Redlands (Commercial bldg)	7	1253	Redlands, 13 Feb. 2010	0.0255	0.026
038	San Bernardino (Office bldg)	3	496	Whittier, 1 Oct. 1987	0.029	0.024
039	South San Francisco (Office bldg)	4	726	Morgan Hill, 24 April 84	0.03	0.02
040	Burbank (Commerce bldg)	6	990	Chino Hills, 29 July 2008	0.028	0.029
041	San Bernardino (Hospital)	5	828	Big Bear City, 22 Feb. 2003	0.0125	0.023
042	San Bernardino (Office bldg)	3	496	Calexico, 04 April 2010	0.0221	0.0179
043	Long Beach (Gov. Office bldg)	15	3456	Chino Hills, 29 July 2008	0.013	0.021
044	San Bernardino (Office bldg)	3	496	Borrego Springs, 07 July 2010	0.0179	0.0169
045	Lancaster (Hospital)	5	942	Big Bear City, 22 Feb. 2003	0.009	0.008
046	San Diego (Commercial bldg)	22	3804	Borrego Springs, 07 Jul. 2010	0.0155	0.0157
047	Los Angeles (Residential bldg)	32	4214	Inglewood, 17 May 2009	0.008	0.0155
048	Gilroy (Hospital)	2	372	San Martin, 15 June 2006	0.016	0.012
049	Richmond (Office bldg)	3	554	Piedmont, 20 July 2007	0.015	0.013
050	Redlands (Commercial bldg)	7	1253	Calexico, 04 April 2010	0.0112	0.0125

473

474

475

476 **Table 2.** Comparison of overturning risk from the considered formulations: the simplified
477 (Kaneko and Hayashi), the direct integration (Housner) and the proposed one. Buildings ID 003,
478 ID 004 and ID 005.

Story	*CHANNEL*	*Simplified*	*Direct integration*	*Proposed*
		ID 003		
1	ACCCHAN2	0%	29%	35%
1	ACCCHAN3	0%	37%	27%
1	ACCCHAN4	0%	36%	36%
3	ACCCHAN5	65%	48%	69%
3	ACCCHAN6	14%	53%	54%
3	ACCCHAN7	65%	71%	69%
4	ACCCHAN8	10%	83%	87%
4	ACCCHAN9	2%	100%	79%
4	ACCCHAN10	100%	99%	92%
		ID 004		
5	ACCCHAN2	96%	100%	82%
5	ACCCHAN3	1%	100%	75%
5	ACCCHAN4	30%	71%	60%
3	ACCCHAN5	4%	77%	47%
3	ACCCHAN6	0%	59%	44%
2	ACCCHAN7	0%	37%	40%
2	ACCCHAN8	0%	40%	34%
5	ACCCHAN10	18%	100%	90%
3	ACCCHAN11	41%	77%	63%
2	ACCCHAN12	2%	56%	45%
		ID 005		
1	ACCCHAN4	0%	42%	23%
1	ACCCHAN5	0%	45%	34%
2	ACCCHAN6	4%	59%	48%

2	ACCCHAN7	0%	50%	37%
2	ACCCHAN8	10%	71%	52%
5	ACCCHAN9	99%	100%	89%
5	ACCCHAN10	98%	77%	86%
5	ACCCHAN11	100%	100%	92%

Table 3. Comparison of the proposed formula and the results of overturning shaking table tests.

Sample	B/H	Overturning PGA from Lab tests & RISK from the new formula					
		Mean [g]	OR	Max [g]	OR	Min [g]	OR
AL1	0.32	0.41	0.66	0.58	0.82	0.23	0.36
AL2	0.14	0.19	0.67	0.24	0.76	0.14	0.58
W1	0.32	0.43	0.68	0.58	0.82	0.23	0.36
W2	0.14	0.18	0.66	0.25	0.77	0.1	0.50
W3	0.39	0.5	0.67	0.61	0.76	0.4	0.55
G	0.39	0.52	0.69	0.73	0.81	0.41	0.56
IB0	0.30	0.49	0.78	0.9	0.87	0.33	0.57
IB2	0.21	0.34	0.76	0.5	0.94	0.23	0.59
IB4	0.28	0.39	0.69	0.76	0.93	0.24	0.45

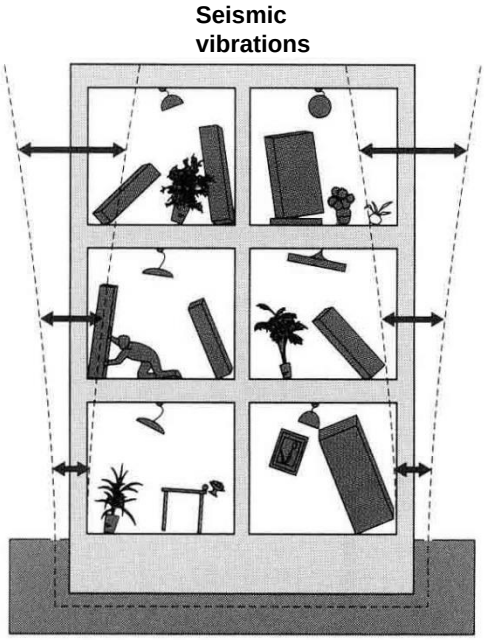

(a)

(b)

(c)

Fig. 1. (a) Overturned furniture and falling flying objects examples. (b,c) Experiences in Mirandola during 2012 Emilia Earthquake, Italy (Cimellaro et al., 2012; 2014).

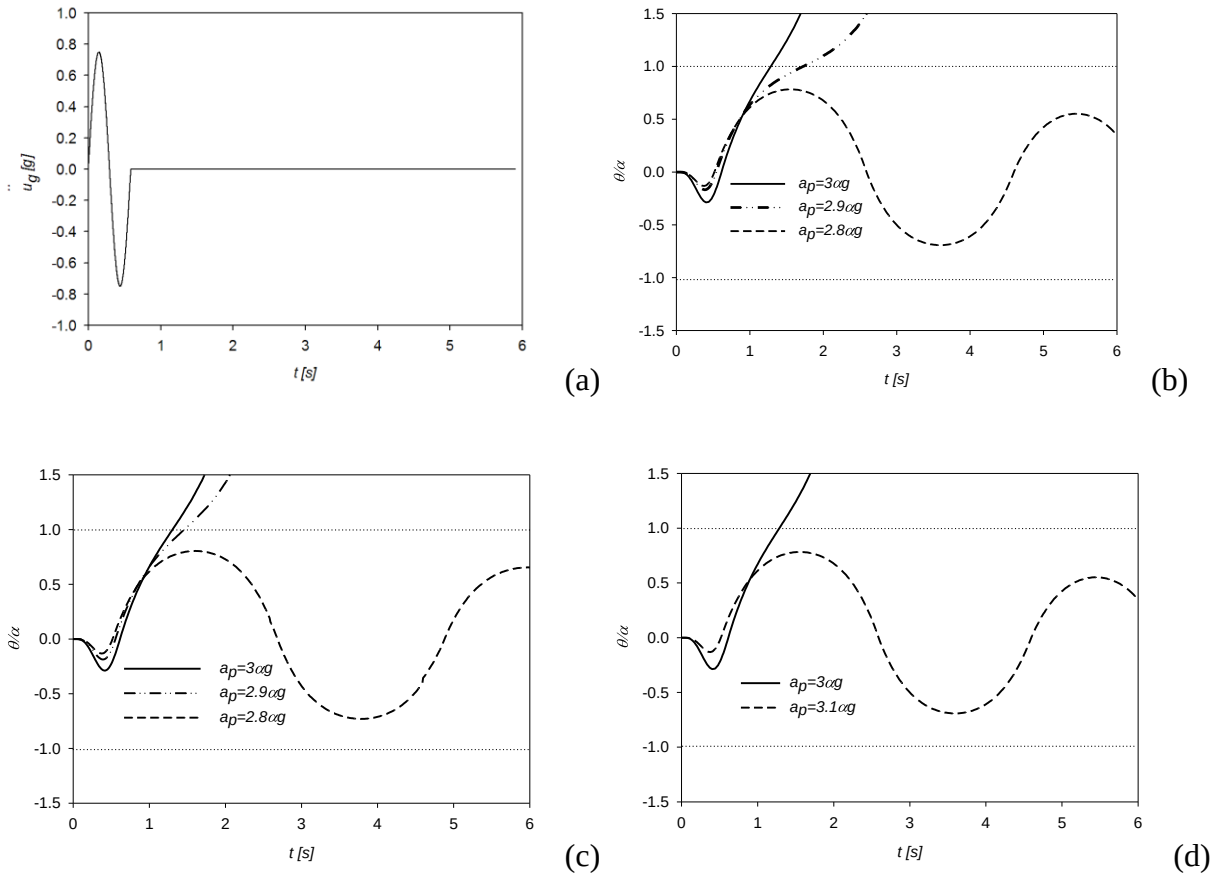

Fig. 2. Comparison of the numerical results of Housner's model subjected to a sinusoidal input using different integration methods: (a) input, (b) ODE45, (c) ODE23s, (d) Zhang and Makris (2001).

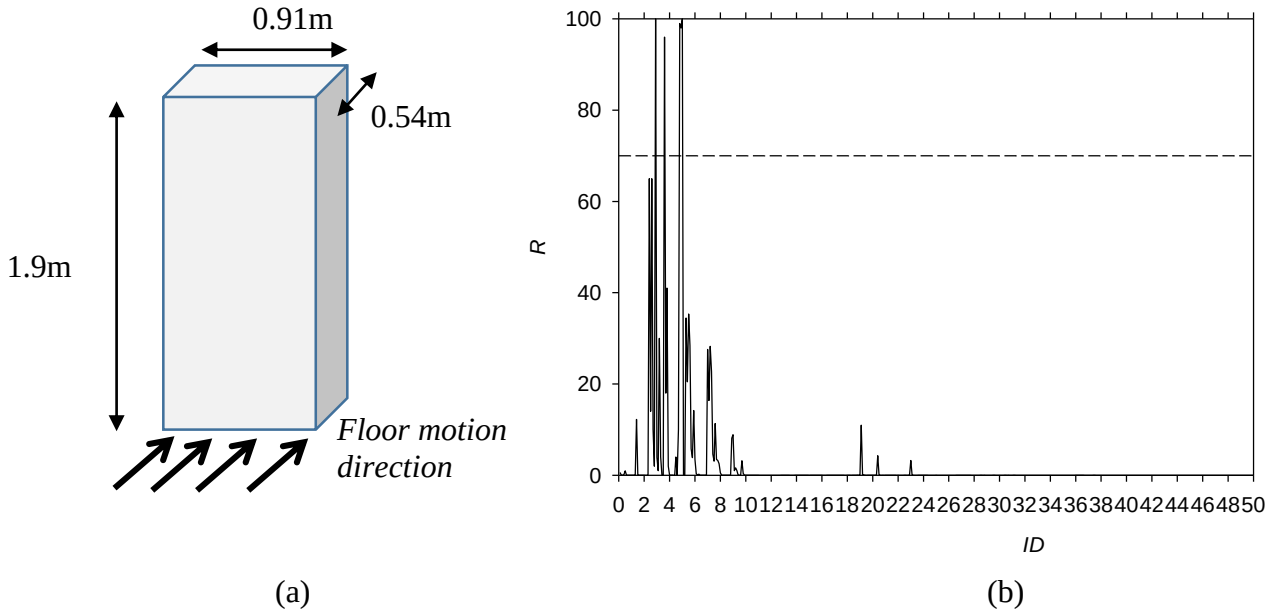

(a) (b)

Fig. 3. Geometry of furniture and floor motion direction (a). Overturning risk results (b) from Kaneko and Hayashi (2004).

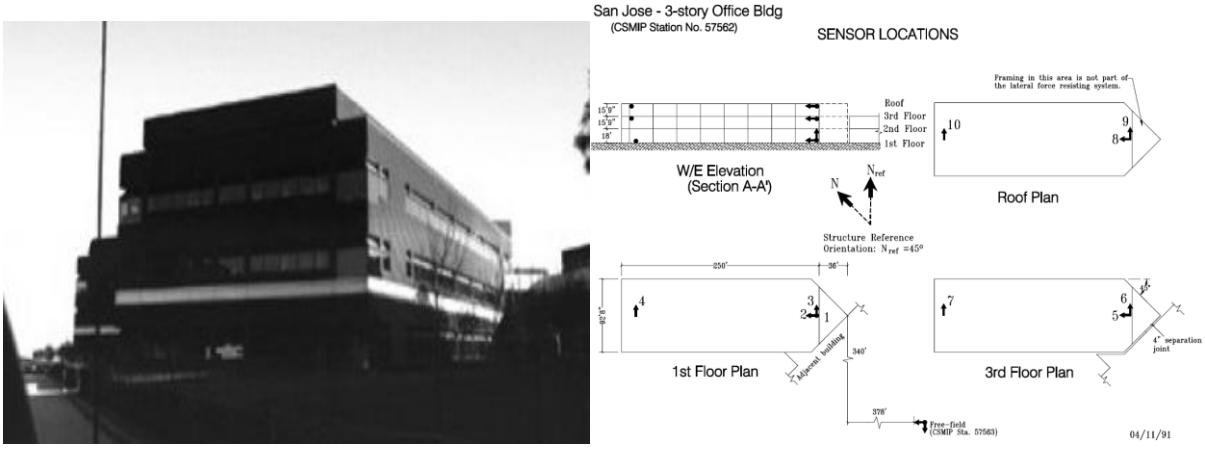

518 (a)

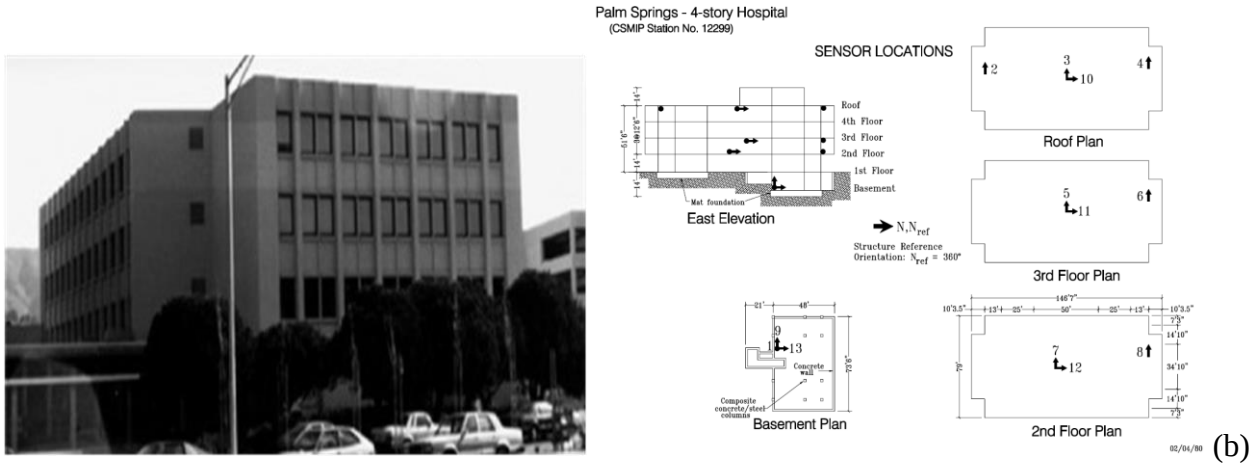

519 (b)

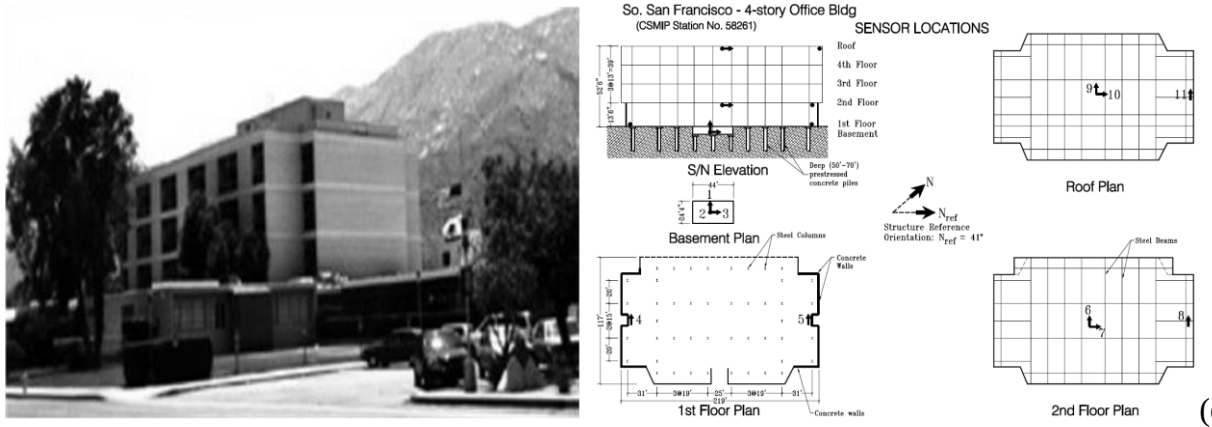

520 (c)

521 **Fig. 4.** San Josè 3-story office building ID 003 (a), Palm Spring 4-story hospital ID 004 (b), South

522 San Francisco 4-story office building ID 005 (c).

523

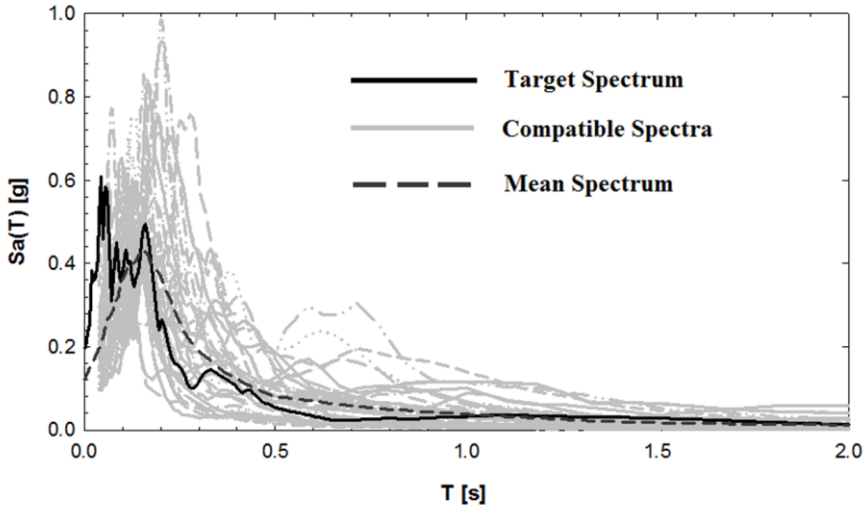

524

525 **Fig. 5.** Spectrum compatible ground motion input used in the Montecarlo analysis.

526
527

528

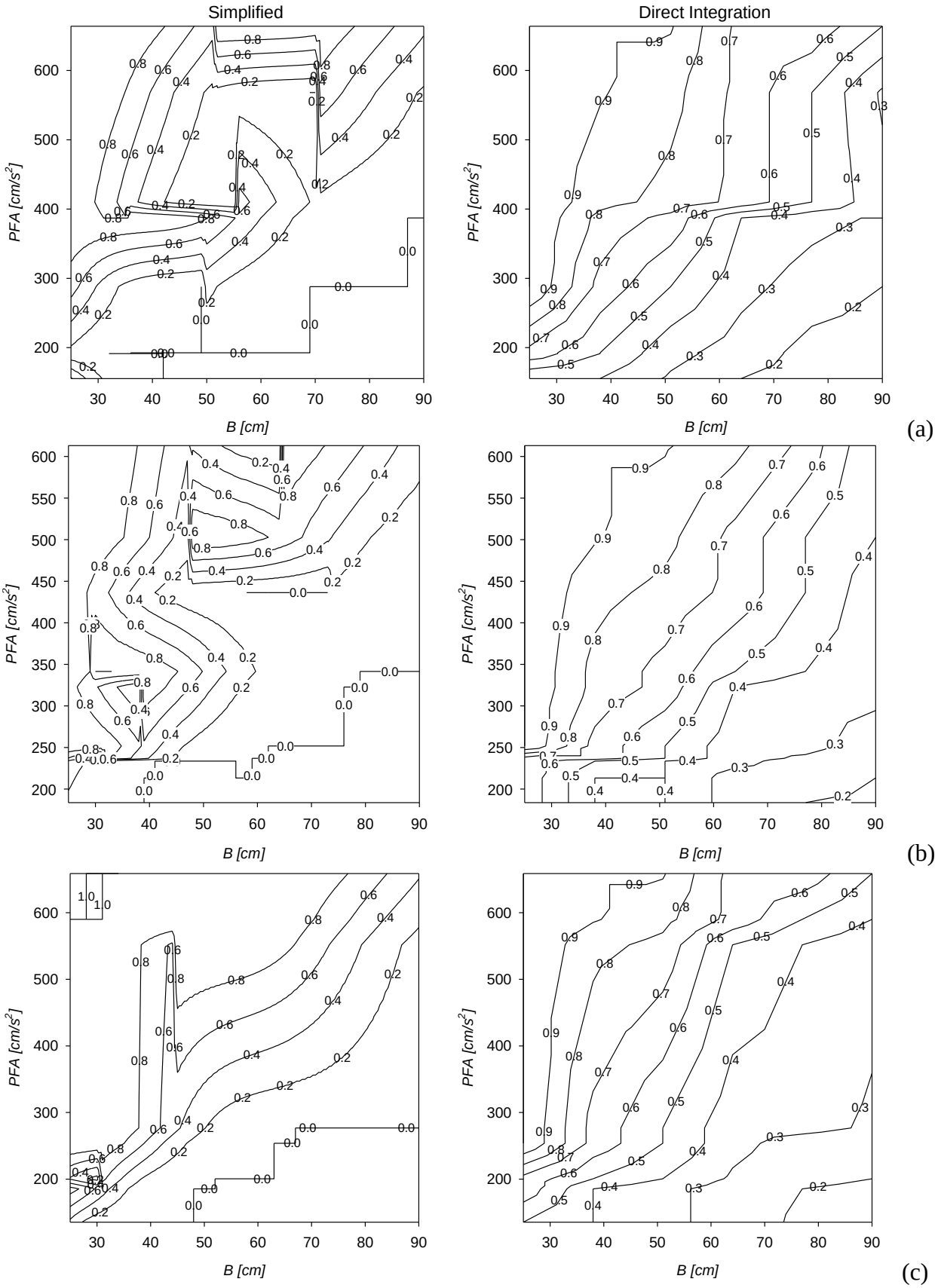

Fig. 6. Comparison of overturning risk *R* between the simplified approach (left) and the direct integration analysis (right) for different furniture slenderness. San Josè 3-story office building ID 003 (a), Palm Spring 4-story hospital ID 004 (b), South San Francisco 4-story office building ID 005 (c).

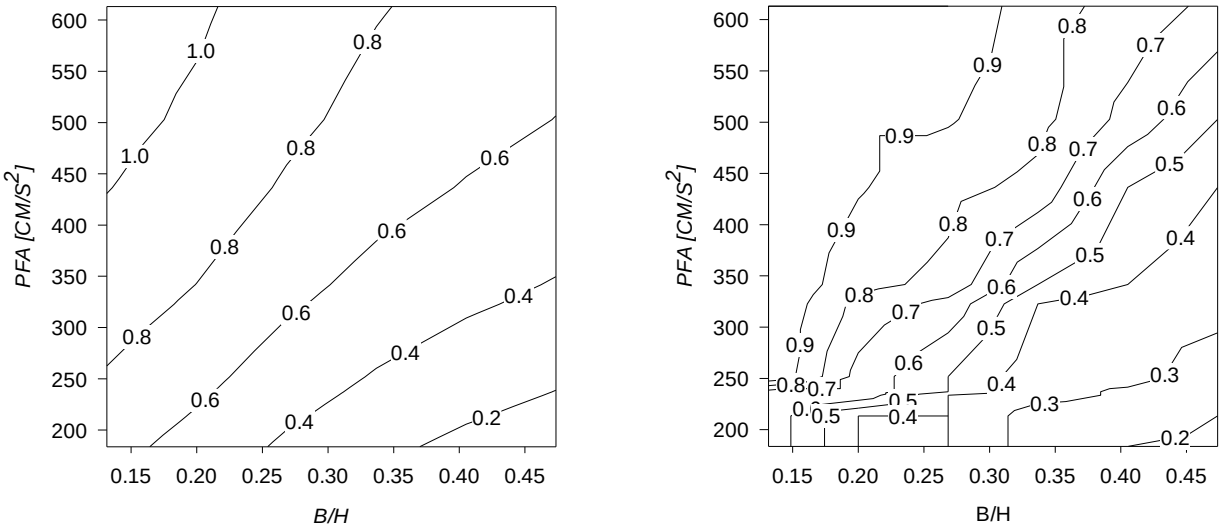

(a) (b)

Fig. 7. Comparison between the results of the proposed formula (a) and the Housner's model (b).

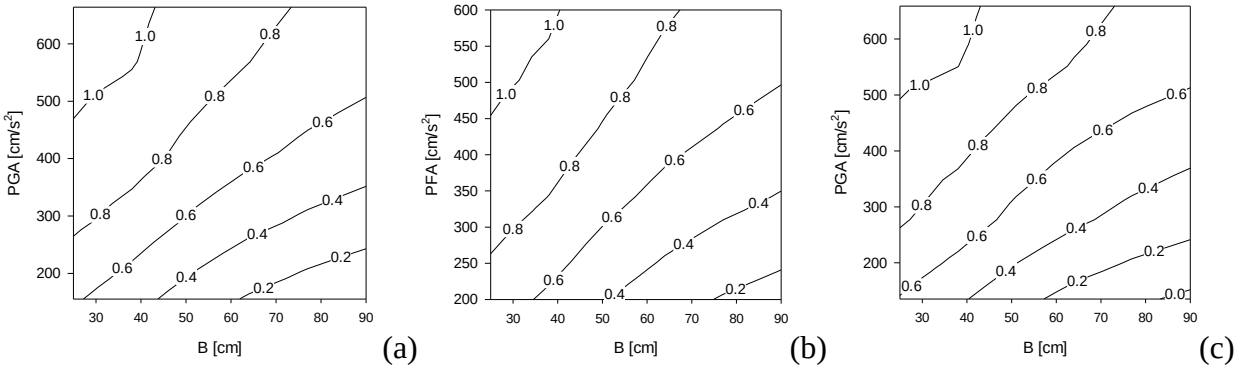

Fig. 8. Overturning risk R from the proposed formulation. San Josè building ID 003 (a), Palm Spring hospital ID 004 (b), South San Francisco building ID 005 (c).